

# DEUTSCHES ELEKTRONEN – SYNCHROTRON

DESY 93-056

April 1993



## A Test of the Lorentz Structure of Semi-Hadronic $\tau$ Decays

H. Thurn, H. Kolanoski

*Institut für Physik, Universität Dortmund*

ISSN 0418-9833

**NOTKESTRASSE 85 · D - 2000 HAMBURG 52**

DESY behält sich alle Rechte für den Fall der Schutzrechtserteilung und für die wirtschaftliche Verwertung der in diesem Bericht enthaltenen Informationen vor.

DESY reserves all rights for commercial use of information included in this report, especially in case of filing application for or grant of patents.

To be sure that your preprints are promptly included in the  
HIGH ENERGY PHYSICS INDEX,  
send them to (if possible by air mail):

**DESY  
Bibliothek  
Notkestraße 85  
W-2000 Hamburg 52  
Germany**

**DESY-IfH  
Bibliothek  
Platanenallee 6  
O-1615 Zeuthen  
Germany**

# A Test of the Lorentz Structure of Semi-Hadronic $\tau$ Decays

H. Thurn and H. Kolanoski

Institut für Physik ; Universität Dortmund, W-4600 Dortmund, Germany

(to be published in Zeitschrift für Physik C)

## Abstract

A method is proposed for the determination of the Lorentz structure of the electroweak interaction in semi-hadronic  $\tau$  decays. Spin correlations in the process

$$e^+e^- \rightarrow \tau^+\tau^- \rightarrow \bar{\nu}_\tau \pi^+ \pi^0 \nu_\tau \pi^- \pi^0 \quad (1)$$

are exploited for a measurement of the normalized product,  $\gamma_{AV} = \frac{2 \operatorname{Re}\{g_A g_V^*\}}{|\bar{g}_V|^2 + |g_A|^2}$ , of the vector ( $g_V$ ) and axial vector ( $g_A$ ) coupling of the  $\tau$  lepton. The contribution of scalar ( $g_S$ ) or pseudo-scalar ( $g_P$ ) couplings is also investigated. Since in the above process the direction of flight of the  $\tau$  leptons can be reconstructed up to a twofold ambiguity a likelihood method using the whole kinematic information can be employed. The matrix element entering the likelihood function has been evaluated in terms of the momenta and angles of the observed pions. The sensitivity of the derived method in an  $e^+e^-$  energy region around 10 GeV has been investigated for the ARGUS experiment using Monte Carlo simulations.

## 1 Introduction

The properties of the third lepton family, the  $\tau$  lepton and the  $\tau$  neutrino, has extensively been studied at  $e^+e^-$  colliders, where  $\tau$  pairs are abundantly produced in  $e^+e^-$  annihilation processes [1]. Although there are still some inconsistencies in the measured  $\tau$ -decay branching ratios it appears now that the experimental results converge towards the expectations from the Standard Model, i.e. the  $\tau$  production and decay seems to be governed by the same electroweak couplings as those determined for the first and second lepton families [2].

While the majority of the measurements concern decay branching ratios the most promising way to search for physics beyond the Standard Model probably lies in a detailed investigation

\*Supported by the German Bundesministerium für Forschung und Technologie, under contract number 054D051P.

of the Lorentz structure of the  $\tau$  decays. Due to the relatively large  $\tau$  mass new couplings (with other than V-A structure) may influence  $\tau$  decays more sensitively than those of the lighter charged leptons. Previous measurements of the Lorentz structure include the determination of the Michel parameters in purely leptonic decays [3]. In semi-hadronic decays the polarisation of the two-pion final state [4] and the parity violation in the three-pion final state have been measured [5]. From the latter experiment the ARGUS collaboration found the helicity of the  $\tau$  neutrino to be left-handed.

In this paper we propose a method for a determination of the normalized product of the vector ( $g_V$ ) and axial vector ( $g_A$ ) decay constants of the  $\tau$  lepton,

$$\gamma_{AV} = \frac{2 \operatorname{Re}\{g_A g_V^*\}}{|\bar{g}_V|^2 + |g_A|^2} \quad (1)$$

A precise measurement of the absolute value of  $\gamma_{AV}$  becomes possible by exploiting spin correlations in  $\tau^+\tau^-$  events where both  $\tau$  leptons decay semi-hadronically. The electroweak production of  $\tau$  pairs in  $e^+e^-$  colliders leads to correlations between the spins of both  $\tau$  leptons, which become observable in the angular correlations between the final state hadrons. E.g. in the case of a vanishing  $\tau$  mass the  $\tau$  leptons have always opposite helicities, resulting in strong correlations between the decay products of the  $\tau$  leptons. Because of experimental advantages — a large branching ratio of about 23% and a high detection efficiency for the decay  $\tau^- \rightarrow \pi^- \pi^0 \nu_\tau$  — we focus our discussion on the following reaction:

$$e^+e^- \rightarrow \tau^+\tau^- \rightarrow \bar{\nu}_\tau \pi^+ \pi^0 \nu_\tau \pi^- \pi^0 \quad (2)$$

Figure 1 shows the Born graph of the complete process and the investigated couplings.

The matrix element of the reaction (2) has previously been worked out in a Lorentz invariant formalism by J.H. Kühn and F. Wagner [6] and is included in the KORALB [7] and KORALZ [8] event generators which are widely used to simulate  $\tau$  production and decays. Here we evaluate the matrix element in terms of measurable momenta and angles of the final state hadrons allowing to reveal in an experimentally more accessible way the dependencies on the coupling parameters  $g_V$  and  $g_A$  as well as of possible non-standard scalar couplings  $g_S$  and  $g_P$ .

The explicit formula for the matrix element is derived in section 2. The maximal exploitation of this formula requires the knowledge of the event axis defined by the direction of flight of the  $\tau$  leptons. The reconstruction of this event axis, up to a twofold ambiguity, is described in section 3. In section 4, a determination of  $\gamma_{AV}^2$  using a likelihood method is proposed and Monte Carlo studies of the sensitivity of the procedure are discussed for the case of the ARGUS experiment [9].

An application to data of the ARGUS experiment will be published in a forthcoming paper by the collaboration. According to the intended application we concentrate in this paper on  $\tau$ -pair production via one-photon exchange. The extension to  $Z^0$  exchange is sketched in appendix A.

## 2 The Calculation of the Matrix Element

The calculation of the matrix element for reaction (2) is divided into three parts. First, the production amplitude  $P_{\lambda_+ \lambda_-}^{\lambda_+ \lambda_-}(e^+e^- \rightarrow \tau^+\tau^-)$  is derived depending on the lepton helicities  $\lambda_i$ .

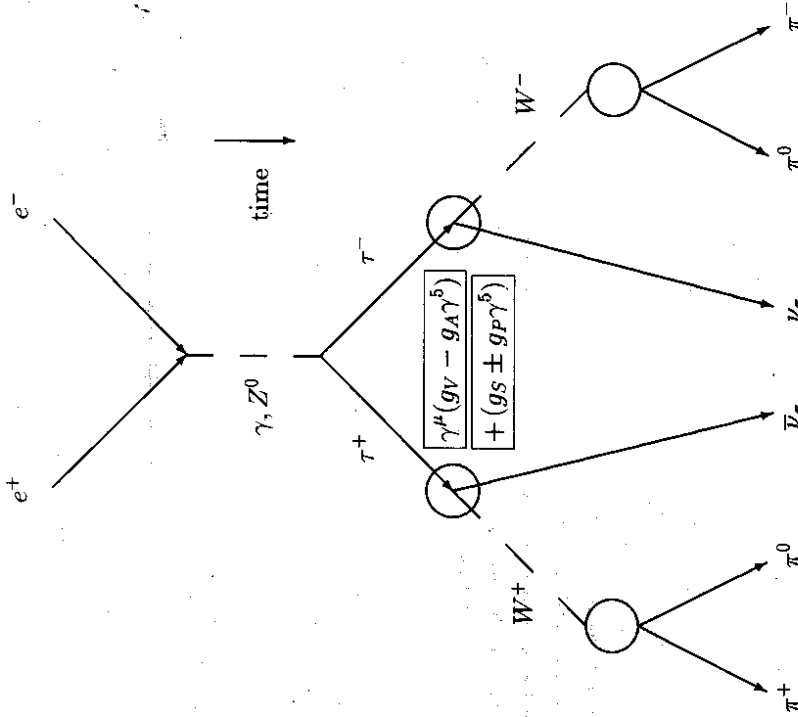


Figure 1: Diagram for the reaction  $e^+e^- \rightarrow \tau^+\tau^- \rightarrow \bar{\nu}_\tau \pi^+ \pi^0 \nu_\tau \pi^- \pi^0$  and the investigated couplings.

Next, the decay amplitudes for the  $\tau^-$  lepton  $D_{\lambda_\tau}^{\lambda_\tau}(\tau^- \rightarrow \pi^- \pi^0 \nu_\tau)$  and correspondingly for the  $\tau^+$  lepton for the different lepton helicities are calculated. Finally, the full matrix element is constructed from the production and decay amplitudes according to:

$$M[e^+(\lambda_+)e^-(\lambda_-) \rightarrow \tau^+(\lambda_+)\tau^-(\lambda_-) \rightarrow \bar{\nu}_\tau(\lambda_{\bar{\nu}_\tau})\pi^+\pi^0 \nu_\tau(\lambda_{\nu_\tau})\pi^-\pi^0] = \quad (3)$$

$$P_{\lambda_+\lambda_+}^{\lambda_+\lambda_-}(e^+e^- \rightarrow \tau^+\tau^-) D_{\lambda_{\nu_\tau}}^{\lambda_{\nu_\tau}}(\tau^- \rightarrow \pi^- \pi^0 \nu_\tau) D_{\lambda_{\bar{\nu}_\tau}}^{\lambda_{\bar{\nu}_\tau}}(\tau^+ \rightarrow \pi^+ \pi^0 \bar{\nu}_\tau)$$

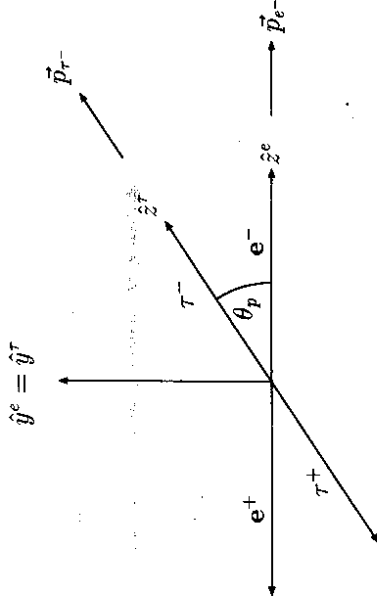


Figure 2: Definition of the two laboratory systems  $FR_{lab}^+$  and  $FR_{lab}^-$ .

## 2.1 The Production Amplitude

The production of  $\tau$  pairs in  $e^+e^-$  annihilations can be represented by the Feynman diagram depicted in the upper part of fig. 1. The corresponding production amplitude is in general a sum of the photon and  $Z^0$  contribution:

$$P(e^+e^- \rightarrow \tau^+\tau^-) = P(e^+e^- \rightarrow \gamma \tau^+\tau^-) + P(e^+e^- \rightarrow Z^0 \tau^+\tau^-)$$

As already mentioned in the introduction we want to concentrate on the application to ARGUS data taken at  $e^+e^-$  energies  $\sqrt{s} \approx 10$  GeV and therefore we restrict ourselves to the one-photon exchange diagram. For these energies the  $Z^0$  contribution to the amplitude which is described in appendix A can be neglected. At higher energies the  $Z^0$  exchange causes the spins of the two  $\tau$  leptons to be not only correlated but also partly polarized.

The production amplitude for the one-photon exchange is given by:

$$P_{\lambda_+\lambda_+}^{\lambda_+\lambda_-}(e^+e^- \rightarrow \tau^+\tau^-) = \frac{ie^2}{s} k_{\lambda_+\lambda_+}^\mu k_{\lambda_+\lambda_-}^\nu g_{\mu\nu} \bar{u}_{\lambda_+}(\vec{p}_{\tau^+}) \gamma^\mu v_{\lambda_+}(\vec{p}_{\tau^+}) \gamma^\nu \bar{u}_{\lambda_-}(\vec{p}_{\tau^-}) \gamma^\nu v_{\lambda_-}(\vec{p}_{\tau^-}) \quad (4)$$

We want to evaluate the leptonic currents,  $k_{\lambda_+\lambda_+}$  and  $k_{\lambda_+\lambda_-}$ , in special laboratory systems,  $FR_{lab}^+$  and  $FR_{lab}^-$ , respectively, choosing the z axis of  $FR_{lab}^+$  in the  $e^-$  flight direction ( $\vec{p}_{lab}^-$ ) and the z axis of  $FR_{lab}^-$  in the  $\tau^-$  flight direction ( $\vec{p}_{lab}^-$ ). The transformation is obtained by rotating  $\hat{z}^+$  into  $\hat{z}^-$  about the common y axis by the production angle  $\theta_p$  (see fig. 2).

In the laboratory system  $FR_{lab}^+$  the electron currents  $k_{\lambda_+\lambda_+}$  for the different lepton helicities are:

$$k_{+-} = \sqrt{s} \begin{pmatrix} 0 \\ 1 \\ -i \\ 0 \end{pmatrix}; \quad k_{-+} = \sqrt{s} \begin{pmatrix} 0 \\ 1 \\ i \\ 0 \end{pmatrix}; \quad k_{++} = 2m_e \begin{pmatrix} 0 \\ 0 \\ 0 \\ 1 \end{pmatrix} = -k_{--}$$

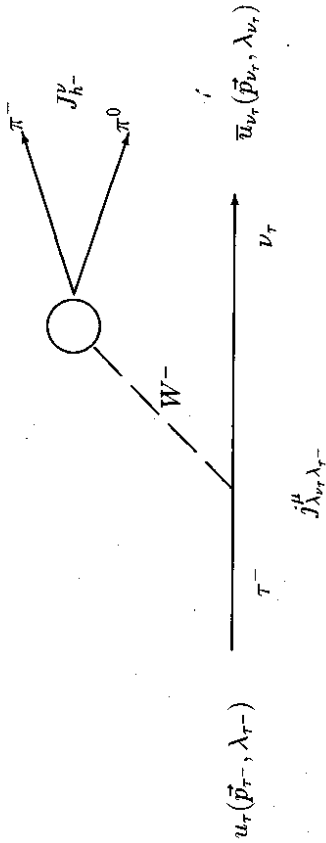


Figure 3: Diagram for the  $\tau^-$  decay

With the approximation  $m_e \ll E_e$ , which will be used henceforth,  $k_{++}$  and  $k_{--}$  vanish. Similarly the  $\tau$ -lepton currents  $l_{\lambda_+ \lambda_-}$  in the laboratory system  $FR_{lab}^-$  are:

$$l_{+-} = \sqrt{s} \begin{pmatrix} 1 \\ 1 \\ i \\ 0 \end{pmatrix}; \quad l_{-+} = \sqrt{s} \begin{pmatrix} 0 \\ 1 \\ -i \\ 0 \end{pmatrix}; \quad l_{++} = 2m_\tau \begin{pmatrix} 0 \\ 0 \\ 0 \\ 1 \end{pmatrix} = -l_{--}. \quad (5)$$

Including a rotation  $R_6^\mu(\theta_p)$  of the electron current into the  $\tau$  frame, the production amplitude

$$P_{\lambda_+ \lambda_- \lambda_e}^{\lambda_+ \lambda_-}(\theta_p) = \frac{ie^2}{s} R_6^\mu(\theta_p) k_{\lambda_e \lambda_e}^\mu g_{\mu\nu} l_{\lambda_+ \lambda_-}^\nu \quad (6)$$

for the different lepton helicities can be written:

$$P_{+-}^{+-}(\theta_p) = ie^2(\cos\theta_p + 1) = P_{-+}^{-+}(\theta_p) \quad (7)$$

$$P_{-+}^{-+}(\theta_p) = ie^2(\cos\theta_p - 1) = P_{+-}^{+-}(\theta_p) \quad (8)$$

$$P_{++}^{++}(\theta_p) = ie^2 \frac{1}{\gamma} \sin\theta_p = P_{--}^{--}(\theta_p) \quad (9)$$

$$P_{--}^{--}(\theta_p) = -ie^2 \frac{1}{\gamma} \sin\theta_p = P_{++}^{++}(\theta_p). \quad (9)$$

Notice that in the approximation  $m_e = 0$   $e^+$  and  $e^-$  occur only with opposite helicities. Furthermore,  $\tau^+ \tau^-$  are produced preferentially with opposite helicities, equal helicities are suppressed by  $1/\gamma = (2m_e)/\sqrt{s}$ . Here we see the basic reason for the occurrence of spin correlations in  $\tau^+ \tau^-$  production.

## 2.2 The Decay Amplitudes

The Feynman diagram of the  $\tau^-$  decay,  $\tau^- \rightarrow \pi^- \pi^0 \nu_\tau$ , is shown in fig. 3. In the four fermion interaction approximation (valid for  $m_{\pi^0} \ll m_W$ ) the corresponding decay amplitude can be

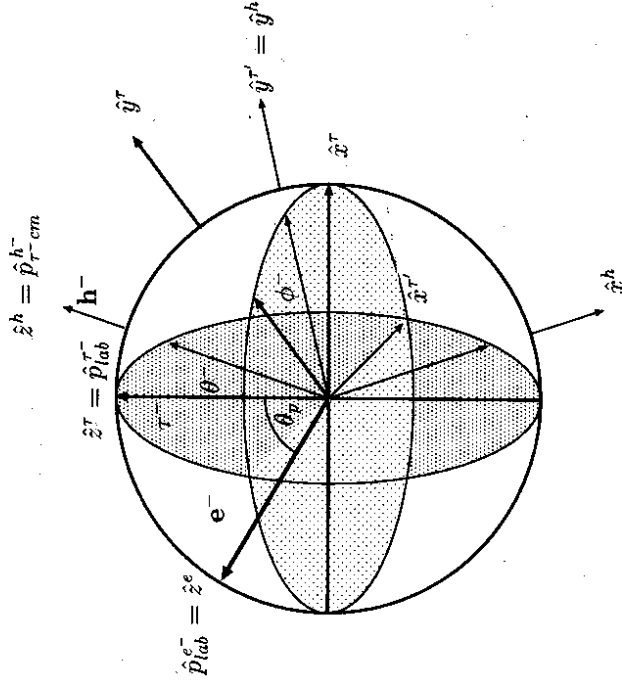


Figure 4: Transformation from the laboratory system  $FR_{lab}^-$  into the  $\tau^-$  c.m. system  $FR_{\tau^- cm}^h$ : After a boost in  $\hat{z}^e$  direction follows a rotation with the azimuthal angle  $\phi^-$  around  $\hat{z}^e$  and the polar angle  $\theta^-$  around  $\hat{y}^e$ .

written as a product of the leptonic current  $j_{\lambda_e \lambda_e}^\mu$  and the hadronic current  $J_h^\nu$  (here the hadronic ( $\pi^- \pi^0$ ) system is called  $h^-$ ):

$$D_{\lambda_e \lambda_e}^{\lambda_+ \lambda_-}(\tau^- \rightarrow \pi^- \pi^0 \nu_\tau) = \frac{G_F}{\sqrt{2}} j_{\lambda_e \lambda_e}^\mu g_{\mu\nu} J_h^\nu. \quad (10)$$

We begin with the calculation of the leptonic current  $j_{\lambda_e \lambda_e}^\mu$ . Under the assumption of a vector-like coupling the current is:

$$j_{\lambda_e \lambda_e}^\mu = \bar{u}_\nu(\vec{p}_\nu, \lambda_\nu) \gamma^\mu (g_V - g_A \gamma^5) u_\tau(\vec{p}_\tau, \lambda_\tau), \quad (11)$$

where in the Standard Model the strength of the vector and axial vector coupling is expected to be equal:  $g_V = g_A = 1$ .

The leptonic and hadronic currents will be calculated in the  $\tau^-$  c.m. system  $FR_{\tau^- cm}^h$  with the  $z$  axis,  $\hat{z}^h$ , chosen in the  $h^-$  flight direction in the  $\tau^-$  c.m. system ( $\vec{p}_{\tau^- cm}^h$ ) and the  $y$  axis perpendicular to the ( $\tau^- \rightarrow h^- \nu_\tau$ ) decay plane (see fig. 4). In this system the neutrino spinor  $\bar{u}_\nu$ , can simply be written ( $m_\nu = 0$ ):

$$\bar{u}_\nu(\vec{p}_\nu, \lambda_\nu) = \sqrt{E_\nu} [\chi^\dagger(-\lambda_\nu), -\lambda_\nu \chi^\dagger(-\lambda_\nu)] \quad (12)$$

with  $\chi^T(1) = (1, 0)$  and  $\chi^T(-1) = (0, 1)$ .

The  $\tau$  spinor, which has a simple representation in the  $\tau$  laboratory system  $FR_{lab}^{\tau}$ :

$$u_{\tau}(\vec{p}_{\tau}, \lambda_{\tau-}) = \sqrt{E_{\tau} + m_{\tau}} \begin{bmatrix} \chi(\lambda_{\tau-}) \\ \frac{|\vec{p}_{\tau}|}{E_{\tau} + m_{\tau}} \lambda_{\tau-} \chi(\lambda_{\tau-}) \end{bmatrix} \quad (13)$$

has to be transformed into  $FR_{\tau-c.m.}^{\tau}$ . Therefore the  $\tau$  spinor is boosted into the  $\tau^-$  c.m. system and rotated into  $FR_{\tau-c.m.}^{h^-}$  with the decay angles  $\theta^-$  and  $\phi^-$ , where  $\theta^-$  is the angle between  $\vec{p}_{\tau}^{\pm}$  and  $\vec{p}_{\tau-c.m.}^{h^-}$  and  $\phi^-$  is the angle between the  $(e^+e^- \rightarrow \tau^+\tau^-)$  production plane and the  $(\tau^- \rightarrow h^- \nu_{\tau})$  decay plane:

$$u_{\tau}^{trans}(\vec{0}, \lambda_{\tau-}) = S_{rot}(\theta^-, \phi^-) S_{Boost} u_{\tau}(\vec{p}_{\tau}, \lambda_{\tau-}) \quad (14)$$

$$= \sqrt{2m_{\tau}} \begin{pmatrix} \cos \frac{\theta^-}{2} \chi(\lambda_{\tau-}) - \lambda_{\tau-} \sin \frac{\theta^-}{2} \chi(-\lambda_{\tau-}) \\ 0 \end{pmatrix} e^{i\lambda_{\tau-} \frac{\phi^-}{2}}.$$

We are now able to evaluate the leptonic currents for the different lepton helicities:

$$j_{\lambda_{\nu_{\tau}} \lambda_{\nu_{\tau}}}^{\mu}(\theta^-, \phi^-) = \bar{u}_{\nu_{\tau}}(\vec{p}_{\nu_{\tau}}, \lambda_{\nu_{\tau}}) \gamma^{\mu} (g_V - g_A \gamma^5) u_{\tau}^{trans}(\vec{0}, \lambda_{\tau-}) \quad (15)$$

$$= \sqrt{2m_{\tau} E_{\nu_{\tau}}} (g_V - g_A \lambda_{\nu_{\tau}}) e^{i\lambda_{\nu_{\tau}} \frac{\phi^-}{2}} V_{\lambda_{\nu_{\tau}} \lambda_{\tau-}}^{\mu}$$

with:

$$V_{\pm\pm} = \begin{pmatrix} \mp \sin \frac{\theta^-}{2} \\ \pm \cos \frac{\theta^-}{2} \\ i \cos \frac{\theta^-}{2} \\ \pm \sin \frac{\theta^-}{2} \end{pmatrix}; \quad V_{\pm\mp} = \begin{pmatrix} \cos \frac{\theta^-}{2} \\ \sin \frac{\theta^-}{2} \\ \pm i \sin \frac{\theta^-}{2} \\ -\cos \frac{\theta^-}{2} \end{pmatrix} \quad (16)$$

To build the hadronic vector current  $J_{h^-}$  the available vectors are  $Q = q_{\pi^-} + q_{\rho^0}$  and  $q = q_{\pi^-} - q_{\rho^0}$ :

$$J_{h^-} = r_1 Q + r_2 q. \quad (17)$$

The Conserved Vector Current hypothesis ( $Q_{\nu} J_{h^-}^{\nu} = 0$ ) requires  $r_1 = -r_2 (qQ)/Q^2$ , which is zero for  $m_{\pi^-} = m_{\rho^0}$ <sup>1</sup>. Taking into account the  $Q^2$  dependence of the hadronic current, one gets:

$$J_{h^-} = \sqrt{2} \cos \theta_c F_{\pi}(Q_-^2) (q_{\pi^-} - q_{\rho^0}) = F_{\pi}(Q_-^2) (q_{\pi^-} - q_{\rho^0}), \quad (18)$$

where  $F_{\pi}(Q^2)$  denotes the pion form factor.

A last frame of reference  $FR_{h^-c.m.}$  is necessary to describe the  $h^-$  decay. This system is the  $h^-$  rest system with the same unit vectors as used in the  $\tau^-$  c.m. system  $FR_{\tau-c.m.}^{h^-}$ . In this system  $q$  is simply:

$$q = \begin{pmatrix} 0 \\ 2\vec{q}_{\pi^-} \end{pmatrix} = 2 |\vec{q}_{\pi^-}| \begin{pmatrix} 0 \\ \sin \alpha^- \cos \beta^- \\ \sin \alpha^- \sin \beta^- \\ \cos \alpha^- \end{pmatrix} \quad (19)$$

<sup>1</sup>The calculation of section 4 has been done without this assumption.

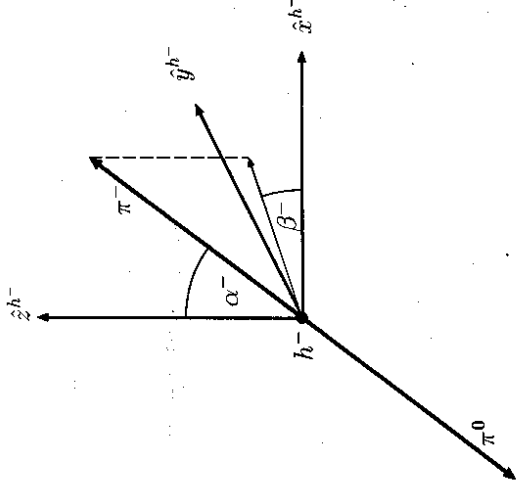


Figure 5: Definition of  $h^-$  decay angles,  $\alpha^-$  and  $\beta^-$ , in the  $h^-$  rest system  $FR_{h-c.m.}$ .

with the decay angles  $\alpha^-$  and  $\beta^-$  defined in fig. 5. Boosting  $q$  into the  $\tau^-$  c.m. system yields the hadronic current in  $FR_{\tau-c.m.}^{h^-}$ :

$$J_{h^-}(\alpha^-, \beta^-) = 2 F_{\pi}(Q_-^2) |\vec{q}_{\pi^-}| \begin{bmatrix} m_{\tau}^2 - Q_-^2 \cos \alpha^- \\ 2m_{\tau} \sqrt{Q_-^2} \sin \alpha^- \cos \beta^- \\ \sin \alpha^- \sin \beta^- \\ m_{\tau}^2 + Q_-^2 \cos \alpha^- \\ 2m_{\tau} \sqrt{Q_-^2} \end{bmatrix} \quad (20)$$

All ingredients are prepared now to calculate the decay amplitude  $D_{\lambda_{\nu_{\tau}}}^{\lambda_{\tau^-}}(\tau^- \rightarrow \pi^- \pi^0 \nu_{\tau})$  for the different lepton helicity combinations:

$$D_{\tau^+}^+ = C_- (g_V - g_A) e^{-i\frac{\phi^-}{2}} \left[ -\frac{m_{\tau}}{\sqrt{Q_-^2}} \sin \frac{\theta^-}{2} \cos \alpha^- - \cos \frac{\theta^-}{2} \sin \alpha^- e^{i\theta^-} \right] \quad (21)$$

$$D_{\tau^+}^- = C_- (g_V - g_A) e^{-i\frac{\phi^-}{2}} \left[ \frac{m_{\tau}}{\sqrt{Q_-^2}} \cos \frac{\theta^-}{2} \cos \alpha^- - \sin \frac{\theta^-}{2} \sin \alpha^- e^{i\theta^-} \right] \quad (22)$$

$$D_{\tau^0}^+ = C_- (g_V + g_A) e^{i\frac{\phi^-}{2}} \left[ \frac{m_{\tau}}{\sqrt{Q_-^2}} \cos \frac{\theta^-}{2} \cos \alpha^- - \sin \frac{\theta^-}{2} \sin \alpha^- e^{-i\theta^-} \right] \quad (23)$$

$$D_{\tau^0}^- = C_- (g_V + g_A) e^{-i\frac{\phi^-}{2}} \left[ \frac{m_{\tau}}{\sqrt{Q_-^2}} \sin \frac{\theta^-}{2} \cos \alpha^- + \cos \frac{\theta^-}{2} \sin \alpha^- e^{-i\theta^-} \right] \quad (24)$$

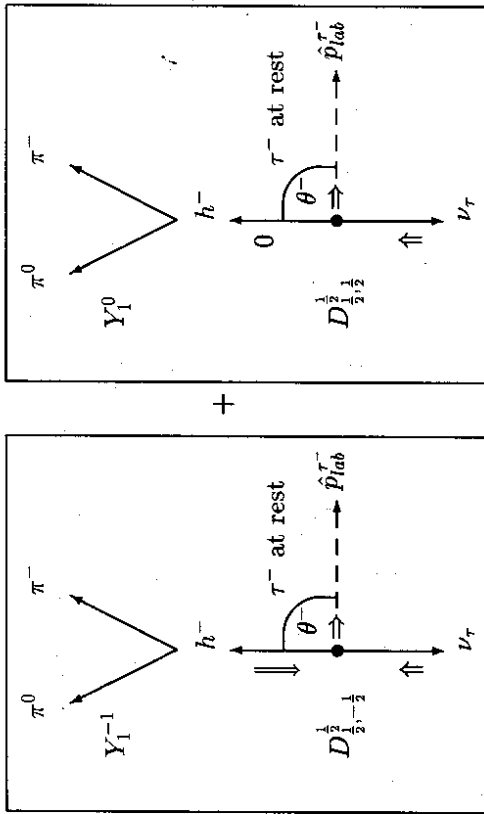


Figure 6: Example for the description of a  $\tau$  decay with the rotation matrices and spherical harmonics

with the helicity independent constant  $C_- = G_F/\sqrt{2} \sqrt{m_\tau^2 - Q_-^2} \sqrt{m_\tau^2 - 4m_\pi^2} F_\pi(Q_-^2)$ . Notice that  $D_+^+$  and  $D_-^+$  vanish for  $g_V = g_A$  as expected from the Standard Model, corresponding to only left-handed coupling for the neutrino.

The angular momentum properties of the  $\pi^- \pi^0$  system (dominated by the  $\rho^-$  resonance) can be best understood by expressing the decay amplitudes (21) to (24) by the rotation matrices  $D_{m, m'}^{j, (\theta^-, \phi^-)}$  ( $m = \lambda_{\tau^-}/2, m' = J_z(h^-) - \lambda_{\nu_e^-}/2$ ) and the spherical harmonics  $Y_{l, l'}^{j, (\theta^-, \phi^-)}$ , e.g.

$$D_{\pm}^{\pm} = \sqrt{\frac{8\pi}{3}} C_{\pm} (g_V + g_A) \left( D_{\frac{1}{2}, -\frac{1}{2}}^{\frac{1}{2}}(\theta^-, \phi^-) Y_1^{-1}(\alpha^-, \beta^-) + \frac{m_\tau}{\sqrt{2} Q_{\pm}^2} D_{\frac{1}{2}, \frac{1}{2}}^{\frac{1}{2}}(\theta^-, \phi^-) Y_1^0(\alpha^-) \right), \quad (25)$$

which is illustrated in fig. 6.

In an analogous way the decay amplitudes  $D_{\lambda_{\nu_e^-}}^{\lambda_{\tau^-}}(\tau^+ \rightarrow \pi^+ \pi^0 \bar{\nu}_e)$  are obtained:

$$D_+^+ = C_+ (g_V + g_A) e^{-i\frac{\phi^+}{2}} \left[ \frac{m_\tau}{\sqrt{Q_+^2}} \cos \frac{\theta^+}{2} \cos \alpha^+ - \sin \frac{\theta^+}{2} \sin \alpha^+ e^{i\beta^+} \right] \quad (26)$$

$$D_-^+ = C_+ (g_V + g_A) e^{i\frac{\phi^+}{2}} \left[ \frac{m_\tau}{\sqrt{Q_+^2}} \sin \frac{\theta^+}{2} \cos \alpha^+ + \cos \frac{\theta^+}{2} \sin \alpha^+ e^{i\beta^+} \right] \quad (27)$$

$$D_{\pm}^{\pm} = C_+ (g_V - g_A) e^{-i\frac{\phi^{\pm}}{2}} \left[ -\frac{m_\tau}{\sqrt{Q_{\pm}^2}} \sin \frac{\theta^{\pm}}{2} \cos \alpha^{\pm} - \cos \frac{\theta^{\pm}}{2} \sin \alpha^{\pm} e^{-i\beta^{\pm}} \right] \quad (28)$$

9

$$D_-^- = C_+ (g_V - g_A) e^{i\frac{\phi^-}{2}} \left[ \frac{m_\tau}{\sqrt{Q_-^2}} \cos \frac{\theta^-}{2} \cos \alpha^- - \sin \frac{\theta^-}{2} \sin \alpha^- e^{-i\beta^-} \right] \quad (29)$$

with the helicity independent constant  $C_+ = G_F/\sqrt{2} \sqrt{m_\tau^2 - Q_+^2} \sqrt{m_\tau^2 - 4m_\pi^2} (F_\pi(Q_+^2))^*$ .

The decay angles  $\phi^+$ ,  $\alpha^+$  and  $\beta^+$  are defined as above for the  $\tau^-$  changing particles to anti-particles with the exception that  $\theta^+$  is the angle between  $\vec{p}_{\tau^+ cm}$  and  $\vec{p}_{\pi^0}^+$ .

Notice that  $D_-^+$  and  $D_-^-$  vanish for  $g_V = g_A$  as expected from the Standard Model, corresponding to only right-handed coupling for the anti-neutrino.

### 2.3 The Matrix Element

The preparation of all ingredients in the previous subsections allows the evaluation of the squared matrix element for the complete process:  $e^+ e^- \rightarrow \tau^+ \tau^- \rightarrow \bar{\nu}_e \pi^+ \pi^0 \nu_\tau \pi^- \pi^0$ . The squared matrix element is given by the squared product of the production amplitude (see 2.1) and the two decay amplitudes (see 2.2) summed coherently over the  $\tau$  helicities ( $\lambda_{\tau^+}, \lambda_{\tau^-}$ ) and incoherently over the neutrino helicities ( $\lambda_{\bar{\nu}_e}, \lambda_{\nu_\tau}$ ) and the  $e^+ e^-$  helicities ( $\lambda_{e^+}, \lambda_{e^-}$ ):

$$|M|^2 = \frac{1}{4} \sum_{\lambda_{e^+}, \lambda_{e^-}, \lambda_{\bar{\nu}_e}, \lambda_{\nu_\tau}} \left| \sum_{\lambda_{\tau^+}, \lambda_{\tau^-}} F_{\lambda_{\tau^+}, \lambda_{\tau^-}}^{\lambda_{e^+}, \lambda_{e^-}} D_{\lambda_{\bar{\nu}_e}}^{\lambda_{\tau^+}} D_{\lambda_{\nu_\tau}}^{\lambda_{\tau^-}} \right|^2 \quad (30)$$

$$= \frac{1}{4} e^4 (|g_V|^2 + |g_A|^2)^2 |C_+ C_-|^2 [\mathbf{A} + \gamma \mathbf{A} \mathbf{B}] \quad (31)$$

$$\mathbf{A} = \left[ 1 + \cos^2 \theta_p + \frac{1}{\gamma^2} \sin^2 \theta_p \right] h_0^+ h_0^- \quad (32)$$

$$\mathbf{B} = - \left[ 1 + \cos^2 \theta_p - \frac{1}{\gamma^2} \sin^2 \theta_p \right] h_1^+ h_1^-$$

$$+ \sin^2 \theta_p \left\{ \cos \Sigma \phi \left[ h_3^+ h_3^- - h_2^+ h_2^- \right] + \sin \Sigma \phi \left[ h_3^+ h_2^- + h_2^+ h_3^- \right] \right\}$$

$$- \frac{1}{\gamma^2} \sin^2 \theta_p \left\{ \cos \Delta \phi \left[ h_3^+ h_3^- + h_2^+ h_2^- \right] + \sin \Delta \phi \left[ h_3^+ h_2^- - h_2^+ h_3^- \right] \right\}$$

$$- \frac{2}{\gamma} \cos \theta_p \sin \theta_p \left[ \sin \phi^+ h_3^+ h_1^- + \sin \phi^- h_1^+ h_3^- \right]$$

$$+ \frac{2}{\gamma} \cos \theta_p \sin \theta_p \left[ \cos \phi^+ h_2^+ h_1^- + \cos \phi^- h_1^+ h_2^- \right]$$

with:

$$h_0^\pm = \frac{m_\tau^2}{Q_\pm^2} \cos^2 \alpha^\pm + \sin^2 \alpha^\pm \quad (33)$$

$$h_1^\pm = -\frac{2m_\tau}{\sqrt{Q_\pm^2}} \cos \alpha^\pm \sin \alpha^\pm \cos \beta^\pm \sin \theta^\pm + \left[ \frac{m_\tau^2}{\sqrt{Q_\pm^2}} \cos^2 \alpha^\pm - \sin^2 \alpha^\pm \right] \cos \theta^\pm \quad (34)$$

$$h_2^\pm = \frac{2m_\tau}{\sqrt{Q_\pm^2}} \cos \alpha^\pm \sin \alpha^\pm \cos \beta^\pm \cos \theta^\pm + \left[ \frac{m_\tau^2}{\sqrt{Q_\pm^2}} \cos^2 \alpha^\pm - \sin^2 \alpha^\pm \right] \sin \theta^\pm \quad (35)$$

$$\begin{aligned}
h_{\pm}^{\pm} &= \frac{2m_{\tau}}{\sqrt{Q_{\pm}^2}} \cos\alpha^{\pm} \sin\alpha^{\pm} \sin\beta_{\pm}^{\pm} \\
\Delta\phi &= \phi^{-} - \phi^{+} \\
\Sigma\phi &= \phi^{+} + \phi^{-}
\end{aligned} \tag{36}$$

This result for the squared matrix element has been numerically compared to the Lorentz invariant expression of reference [6] (see appendix B) and was found to be in exact agreement. A similar comparison with the matrix element calculated in the KORALB program yielded a disagreement which could be cured by rotating all momenta of the  $\tau^{\pm}$  decay particles by an angle  $\pi$  around the  $\tau^{-}$  axis<sup>2</sup>. In the analysis of section 4 we have used this correction.

## 2.4 Addition of Scalar-like Couplings

To include scalar ( $gs$ ) and pseudo-scalar ( $gp$ ) couplings of the  $\tau$  leptons, we have to extend the  $\tau$  decay amplitudes:

$$D_{\lambda_{\nu}^{\pm}}^{\lambda_{\tau}^{\pm}}(\tau^{\pm} \rightarrow \pi^{\pm} \pi^0 \nu_{\tau}) = \frac{G_F}{\sqrt{2}} \left\{ j_{\lambda_{\nu}^{\pm} \lambda_{\tau}^{\pm}}^{\tau} g_{\mu\nu} J_{h_{\pm}^{\pm}}^{\nu} + j_{\lambda_{\nu}^{\pm} \lambda_{\tau}^{\pm}}^{\pi} J_{h_{\pm}^{\pm}}^{\pi} \right\} \tag{37}$$

with:

$$j_{\lambda_{\nu}^{\pm} \lambda_{\tau}^{\pm}}^{\tau} = \bar{u}_{\nu_{\tau}}(\vec{p}_{\nu_{\tau}}, \lambda_{\nu_{\tau}}) (gs + gp\gamma^5) u_{\tau}(\vec{p}_{\tau}, \lambda_{\tau}) \tag{38}$$

$$j_{\lambda_{\nu}^{\pm} \lambda_{\tau}^{\pm}}^{\pi} = \bar{v}_{\tau}(\vec{p}_{\tau}, \lambda_{\tau}) (gs - gp\gamma^5) v_{\nu_{\tau}}(\vec{p}_{\nu_{\tau}}, \lambda_{\nu_{\tau}}) \tag{39}$$

$$J_{h_{\pm}^{\pm}}^{\tau} = f_s(Q_{\pm}^2). \tag{40}$$

Notice that  $gs = gp$  corresponds to only left- (right-) handed coupling for the (anti) neutrino. The addition of scalar-like couplings with these extensions results in a matrix element for reaction (2), which can be obtained from the one for only vector-like couplings by changing in (33) to (36) the definitions of  $h_0^{\pm}$  to  $h_{s0}^{\pm}$ :

$$h_0^{\pm} \rightarrow h_{s0}^{\pm} = h_0^{\pm} + R_{SV}^2 |f_s(Q_{\pm}^2)|^2 \mp \gamma_{AP} |f_s(Q_{\pm}^2)| \frac{m_{\tau}}{\sqrt{Q_{\pm}^2}} \cos\alpha^{\pm} \cos\psi_r \tag{41}$$

$$\begin{aligned}
h_{\pm}^{\pm} \rightarrow h_{s\pm}^{\pm} &= h_{\pm}^{\pm} + R_{SV}^2 \frac{\gamma_{SP}}{\gamma_{AV}} |f_s(Q_{\pm}^2)|^2 \cos\theta^{\pm} \mp \frac{\gamma_{AS}}{\gamma_{AV}} |f_s(Q_{\pm}^2)| \frac{m_{\tau}}{\sqrt{Q_{\pm}^2}} \cos\alpha^{\pm} \cos\theta^{\pm} \cos\psi_r \\
&\pm \sin\alpha^{\pm} \sin\theta^{\pm} \frac{|f_s(Q_{\pm}^2)|}{\gamma_{AV}} \left[ \gamma_{AS} \cos(\psi_r) \cos(\beta_{\pm}^{\pm}) - \gamma_{AP} \sin(\psi_r) \sin(\beta_{\pm}^{\pm}) \right] \tag{42}
\end{aligned}$$

$$h_{\pm}^{\pm} \rightarrow h_{s\pm}^{\pm} = h_{\pm}^{\pm} + R_{SV}^2 \frac{\gamma_{SP}}{\gamma_{AV}} |f_s(Q_{\pm}^2)|^2 \sin\theta^{\pm} \mp \frac{\gamma_{AS}}{\gamma_{AV}} |f_s(Q_{\pm}^2)| \frac{m_{\tau}}{\sqrt{Q_{\pm}^2}} \cos\alpha^{\pm} \sin\theta^{\pm} \cos\psi_r \tag{43}$$

$$\mp \sin\alpha^{\pm} \cos\theta^{\pm} \frac{|f_s(Q_{\pm}^2)|}{\gamma_{AV}} \left[ \gamma_{AS} \cos(\psi_r) \cos(\beta_{\pm}^{\pm}) - \gamma_{AP} \sin(\psi_r) \sin(\beta_{\pm}^{\pm}) \right] \tag{44}$$

$$h_{\pm}^{\pm} \rightarrow h_{s\pm}^{\pm} = h_{\pm}^{\pm} \mp \sin\alpha^{\pm} \frac{|f_s(Q_{\pm}^2)|}{\gamma_{AV}} \left[ \gamma_{AS} \cos(\psi_r) \sin(\beta_{\pm}^{\pm}) + \gamma_{AP} \sin(\psi_r) \cos(\beta_{\pm}^{\pm}) \right] \tag{44}$$

<sup>2</sup>This error of KORALB has meanwhile been confirmed by the authors of the program [1].

with:

$$R_{SV}^2 = \frac{g_S^2 + g_P^2}{g_V^2 + g_A^2} \tag{45}$$

$$\gamma_{SP} = \frac{2g_S g_P}{g_S^2 + g_P^2} \tag{46}$$

$$\gamma_{AS} = \frac{2(g_A g_S + g_V g_P)}{g_V^2 + g_A^2} \tag{47}$$

$$\gamma_{AP} = \frac{2(g_A g_P + g_V g_S)}{g_V^2 + g_A^2} \tag{48}$$

$$f_s(Q_{\pm}^2) = f_s(Q_{\pm}^2) / \left( \sqrt{Q_{\pm}^2 - 4m_{\tau}^2} F'_{\pi}(Q_{\pm}^2) \right) = |f_s(Q_{\pm}^2)| e^{i\psi_{\pi}(Q^2)}. \tag{49}$$

In the equations above we have assumed that  $g_V$  and  $g_A$  as well as  $g_S$  and  $g_P$  are relatively real. A possible phase between the scalar and vector couplings is absorbed in  $f_s(Q_{\pm}^2) = |f_s(Q_{\pm}^2)| e^{i\psi_{\pi}(Q^2)}$  which already has to account for the strong phase of the  $\pi^{\pm} \pi^0$  system. Note that a scalar  $\pi^{\pm} \pi^0$  system cannot originate from a  $q\bar{q}$  state, which would have odd G parity. However, such a final state may be produced from an exotic state with isospin  $I = 2$  or from the decay of a new scalar particle.

## 2.5 Projections of the Differential Cross Section

The general formulas for the matrix element given in the previous subsections allow to calculate several projections of the differential cross sections. Such low-dimensional distributions may render the dependencies on the coupling parameters more transparent. We describe the  $Q^2$  dependence of the hadronic vector current by a narrow-width approximation for a  $\rho$ -resonance:  $|F_{\pi}(Q^2)|^2 \sim \delta(Q^2 - m_{\rho}^2)$ . In the following we have evaluated two projections under the assumption of only vector-like couplings of the  $\tau$  lepton and a third one including scalar-like couplings:

The first projection describes an energy-energy correlation between the two hadron systems ( $\pi^{+} \pi^0$ ) and ( $\pi^{-} \pi^0$ ) and has already been suggested in reference [6]<sup>3</sup>:

$$\frac{1}{\sigma_{\text{tot}}} \frac{d\sigma}{d\cos\theta^{+} d\cos\theta^{-}} = \frac{1}{4} \left[ 1 - \gamma_{AV}^2 \left( \frac{s - 2m_{\tau}^2}{s + 2m_{\rho}^2} \right) \left( \frac{m_{\tau}^2 - 2m_{\rho}^2}{m_{\tau}^2 + 2m_{\rho}^2} \right) \left( \frac{m_{\tau}^2 - 2m_{\rho}^2}{m_{\tau}^2 + 2m_{\rho}^2} \right) \cos\theta^{+} \cos\theta^{-} \right] \tag{50}$$

with:

$$\cos\theta^{\pm} = \frac{4m_{\tau}^2 E_{\rho^{\pm}}^{lab} - \sqrt{s}(m_{\tau}^2 + m_{\rho^{\pm}}^2)}{\sqrt{s - 4m_{\tau}^2}(m_{\tau}^2 - m_{\rho^{\pm}}^2)} \tag{51}$$

and the total cross section  $\sigma_{\text{tot}}$  for reaction (2) without scalar couplings.

As a second projection we have calculated the differential cross section with respect to  $\Sigma\phi = \phi^{+} + \phi^{-}$  (modulo  $2\pi$ ) defined with the azimuth angles  $\phi^{\pm}$  between the  $\tau$  pair production plane and the  $\tau^{\pm}$  decay planes:

$$\frac{1}{\sigma_{\text{tot}}} \frac{d\sigma}{d\Sigma\phi} = \frac{1}{2\pi} \left[ 1 - \gamma_{AV}^2 \frac{\pi^2}{32} \left( \frac{s}{s + 2m_{\rho}^2} \right) \left( \frac{m_{\tau}^2 - 2m_{\rho}^2}{m_{\tau}^2 + 2m_{\rho}^2} \right) \left( \frac{m_{\tau}^2 - 2m_{\rho}^2}{m_{\tau}^2 + 2m_{\rho}^2} \right) \cos\Sigma\phi \right] \tag{52}$$

<sup>3</sup>Our equation (50) is not in agreement with the corresponding eq. (4.13) in reference [6] which is probably due to printing errors in [6].



Hence already the one-dimensional distribution of  $\Sigma\phi$ , which is measurable up to a twofold ambiguity (see section 3), allows in principle a determination of  $\gamma_{AV}^2$ .

When a scalar-like coupling of the  $\tau$  lepton is included, the distribution of the polar angle  $\cos\alpha^\pm$  (defined in fig. 5) shows an asymmetry, which promises a high sensitivity for a determination of  $\gamma_{AP} = 2(g_A g_P + g_V g_S) / (g_V^2 + g_A^2)$ :

$$\frac{1}{\sigma_{tot}} \frac{d\sigma_s}{d\cos\alpha^\pm} = \frac{3}{2m_\tau^2 + 4m_\rho^2} (1 + \frac{3m_\rho^2}{m_\tau^2 + 2m_\rho^2} \frac{R_{SV}^2}{R_{SV}}) \quad (53)$$

Here we assumed a constant  $f_r(Q_\pm^2) = e^{i\psi_r(Q^2)}$ . This simplification can be dropped if the formula is evaluated in bins of  $Q^2$ . Notice that with a vector-like coupling as expected from the Standard Model,  $g_V = g_A = 1$ ,  $\gamma_{AP}$  measures directly  $(g_S + g_P)$  in units of the Fermi coupling constant  $G_F/\sqrt{2}$ .

In section 4 we compare the sensitivities of the projections (50, 52, 53) for a determination of the coupling parameters using the whole kinematical information.

### 3 The Reconstruction of the $\tau$ Axes

Although the detectors at present  $e^+e^-$  colliders are not able to measure directly the flight direction of the  $\tau$  lepton, the kinematical information given by the experimentally observable hadronic decay products of the two  $\tau$  leptons constrains the possible  $\tau$  flight direction up to a twofold ambiguity.

The momentum  $\vec{p}_{h^-}$  of the  $h^-$  is measurable and the values of the  $\tau$  momentum  $|\vec{p}_{\tau^-}|$  and the neutrino momentum  $|\vec{p}_{\nu\tau^-}| = E_{\tau^-} - E_{h^-}$  are also known assuming the  $\tau$  energy  $E_\tau$  is given by the beam energy  $\sqrt{s}/2$ . The resulting triangle of these three momenta fixes the angle  $\theta_{lab}^h$  between the  $h^-$  and the  $\tau^-$  direction in the laboratory:

$$\cos\theta_{lab}^h = \frac{\sqrt{s}(\vec{p}_{h^-}^2 + Q_\tau^2) - m_\tau^2 - Q_\tau^2}{|\vec{p}_{h^-}| \sqrt{s - 4m_\tau^2}} \quad (54)$$

In other words the  $\tau$  direction has to lie on a cone around  $\vec{p}_{h^-}$  with an opening angle  $\theta_{lab}^h$ .

Since the same argument is valid for the decay of the  $\tau^+$  lepton, a second cone can be reconstructed with an opening angle  $\theta_{lab}^+$ . Under the assumption of a back-to-back production of the  $\tau$  pair the two possible  $\tau$  axes correspond to the two intersection lines of the two cones (see fig. 7).

The two possible unit vectors  $\hat{e}_\tau(1,2)$  of the  $\tau^-$  direction are given in the following equation:

$$\hat{e}_\tau(1,2) = a\hat{n}_1 \pm b\hat{n}_2 + c\hat{n}_3 \quad (55)$$

with:

$$\begin{aligned} \hat{n}_1 &= \frac{\vec{p}_{h^-} - \vec{p}_{h^+} \cos\Delta\theta}{\sin\Delta\theta}, & a &= \frac{\cos\theta_{lab}^- + \cos\theta_{lab}^+ \cos\Delta\theta}{\sin\Delta\theta} \\ \hat{n}_2 &= \frac{\vec{p}_{h^-} \times \vec{p}_{h^+}}{\sin\Delta\theta}, & b &= \sqrt{1 - a^2 - c^2} \\ \hat{n}_3 &= -\hat{p}_{h^+}, & c &= \cos\theta_{lab}^+ \end{aligned}$$

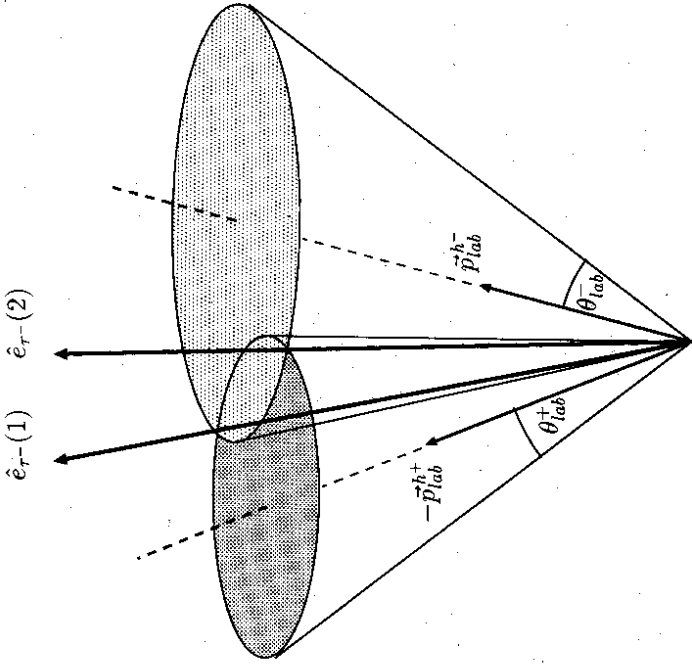


Figure 7: Reconstruction of the  $\tau$  axes up to a twofold ambiguity using the whole kinematical information.

and with:  $\hat{p}_{h^\pm} = \vec{p}_{h^\pm} / |\vec{p}_{h^\pm}|$  and  $\cos\Delta\theta = \hat{p}_{h^+} \cdot \hat{p}_{h^-}$ .

One gets 0, 1 or 2 solutions for the  $\tau$  axes for  $(1 - a^2 - c^2) < 0$ ,  $= 0$  or  $> 0$ , respectively, corresponding to  $\theta_{lab}^+ + \theta_{lab}^- - \Delta\theta < \pi$ ,  $= \pi$  or  $> \pi$ . The case of no reconstructed  $\tau$  axis is only possible due to radiation effects and the finite resolution of the detector.

Figure 8 shows the distributions of the smaller and the larger angle between the real  $\tau$  axis and one of the reconstructed  $\tau$  axes for 1000 Monte Carlo events (details of the event generation in section 4).

### 4 The Sensitivity of a Determination of $\gamma_{AV}^2$ and $\gamma_{AP}$

In this section various methods for a determination of  $\gamma_{AV}^2$  and of  $\gamma_{AP}$  are discussed and the corresponding sensitivities are investigated. First, a likelihood method is described, which exploits the whole kinematical information of the process. The influence of the size of the analysed data sample, the finite resolution of a detector and radiation effects on this procedure have been studied. The sensitivities of a  $\gamma_{AV}^2$  determination using the projections derived in subsection 2.5 are compared with this likelihood method.

events per 1 degree

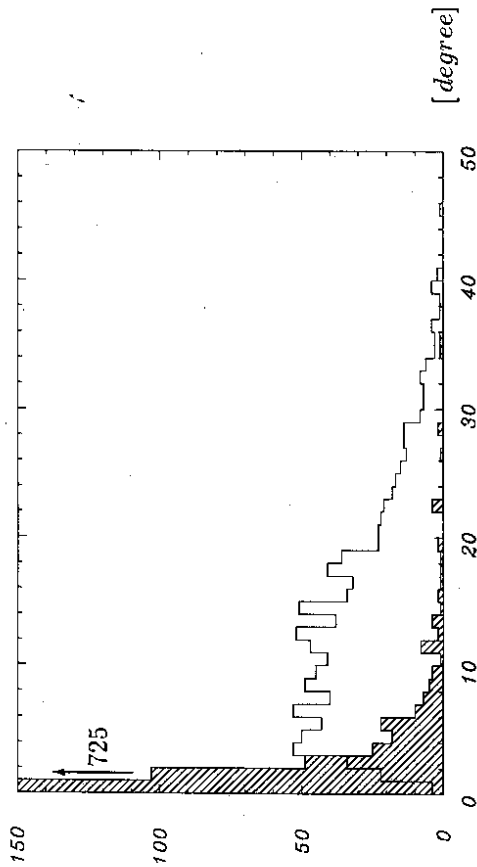


Figure 8: Distribution of the angle between the real and the two reconstructed  $\tau$  axes (without detector effects). The smaller (larger) angle is filled into the hatched (open) histogram. The non-zero entries of the hatched histogram are due to radiation effects.

Since the matrix element  $|M_i(e^+e^- \rightarrow \tau^+\tau^- \rightarrow \bar{\nu}_\tau \pi^+ \pi^0 \nu_\tau \pi^- \pi^0)|^2$  evaluated in section 2 is proportional to the probability  $P_i$  of a given event  $i$ , a likelihood method can be performed to determine the parameter  $\gamma_{AV}^2$ . We sum over the two probabilities  $P_1^i$  and  $P_2^i$  of one event, which belong to the two possible  $\tau$  axes reconstructed in section 3:  $P_i = P_1^i + P_2^i$ . The event is discarded if no  $\tau$  axis can be reconstructed (which can be caused by resolution and radiation effects, see section 3).

With these probabilities  $P_i(\gamma_{AV}^2)$  we can evaluate a likelihood function:

$$L(\gamma_{AV}^2) = \prod_i P_i(\gamma_{AV}^2). \quad (56)$$

The parameter  $\gamma_{AV}^2 = (2 \operatorname{Re}\{g_A g_V^*\}) / (|g_V|^2 + |g_A|^2)$ , running in the allowed region between 0 and 1 ( $\gamma_{AV}^2 > 1$  leads to negative probabilities), is determined by maximising  $L$  with respect to this parameter.

In order to test the sensitivity of the procedure, Monte Carlo events of the reaction (2) have been produced with a center of mass energy  $\sqrt{s} = 10.58$  GeV using the event generator program KORALB (version 2.1) [7]. This event generator includes the full matrix element with all angular correlations and radiation effects. After the correction in KORALB as described in section 2.3, it has been checked that without radiation effects the generator yields results identical to those derived in section 2. Therefore the produced Monte Carlo data can be used to investigate the sensitivity of the proposed analysis method.

As a first test three data samples of 1000 events each were generated without radiation effects and assuming an ideal detector for three different  $\gamma_{AV}^2$  values:  $\gamma_{AV}^2 = 0.0, 0.6$  and 1.0. The resulting likelihood functions are shown as full lines in fig. 9. The method has no problems

to distinguish between the three cases. Taking into account only the real  $\tau$  axis, which is known for Monte Carlo data, the likelihood functions are somewhat narrower (dashed lines in fig. 9).

The finite resolution of a detector requires an acceptance correction of the probabilities  $P_i$  with the acceptance factor  $\eta_{acc}(\vec{\alpha})$ , which depends on all variables  $\vec{\alpha}$  of the phase space:

$$P_i^{corr}(\gamma_{AV}^2; \vec{\alpha}) = \frac{A(\vec{\alpha}) + \gamma_{AV}^2 B(\vec{\alpha})}{I_{norm}} \eta_{acc}(\vec{\alpha}), \quad (57)$$

with:

$$I_{norm} = \int \{A(\vec{\alpha}) + \gamma_{AV}^2 B(\vec{\alpha})\} \eta_{acc}(\vec{\alpha}) d\vec{\alpha}.$$

Notice that the  $\gamma_{AV}^2$  determination is only affected by the normalisation integral of the acceptance correction, since  $\eta_{acc}(\vec{\alpha})$  can be assumed to be independent of  $\gamma_{AV}^2$ .

To investigate the influence of the finite detector resolution and of radiation effects 1000 events with  $\gamma_{AV}^2 = 0.6$  have been generated with and without radiation. For this purpose the Monte Carlo events were fed into the simulation program SIMARG [10], which simulates the ARGUS detector and afterwards the events were reconstructed with the ARGUS reconstruction. With an analysis program [12] the four momenta of the final state hadrons could be calculated, which led to a Monte Carlo data sample including all effects of the detector. The comparison of the resulting likelihood function with the one obtained for an ideal detector (both with radiation effects) is shown in fig. 10. We conclude that neither detector nor radiative effects influence significantly the analysis.

The sensitivity of the  $\gamma_{AV}^2$  determination depending on the number of used events has been studied with two Monte Carlo data samples, including radiation effects, generated with  $\gamma_{AV}^2 = 0.6$  and 1.0. In both cases we have evaluated the likelihood function after each additional event. In the first case the integration of the likelihood function from the position of the maximum into the direction of lower and higher values of  $\gamma_{AV}^2$  yields the  $+\sigma$  and  $-\sigma$  boundaries for  $\gamma_{AV}^2$  depending on the number of used events. In the second case the likelihood function was integrated from  $\gamma_{AV}^2 = 1.0$  to lower values and a lower limit for  $\gamma_{AV}^2$  with a 95% confidence level was evaluated after each additional event.

The two resulting boundaries as a function of the event numbers are shown in fig. 11 and fig. 12. The open points in both figures belong to data taken with an ideal detector, while the full points reflect the influence of a finite detector resolution. Obviously it is advisable to measure somewhat more than 1000 events. With an acceptance of about 10% this corresponds to an integrated luminosity of about  $200 \text{ pb}^{-1}$ .

The determination of  $\gamma_{AV}^2$  is also possible by evaluating the correlation coefficient of the energy-energy correlation (50) or fitting the one-dimensional distribution of  $\Sigma \phi$  (52). The sensitivities of these methods for an ideal detector neglecting radiative effects are studied with a data sample of 2000 events generated with  $\gamma_{AV}^2 = 0.6$ . The comparison with the likelihood method shown in table 1 demonstrates clearly the advantage of using the whole kinematical information.

The projection (53) yields a forward-backward asymmetry with respect to  $\cos\alpha^\pm$ , which promises a high sensitivity for a determination of  $\gamma_{AP}$ :

$$A_{FB} = \frac{N(\cos\alpha^\pm \geq 0) - N(\cos\alpha^\pm \leq 0)}{N(\cos\alpha^\pm \geq 0) + N(\cos\alpha^\pm \leq 0)} = \mp \frac{3m_\tau m_p}{2m_\tau^2 + 4m_p^2} \gamma_{AP} \approx \mp 0.47 \gamma_{AP}, \quad (58)$$

where we have set  $R_{SV}^2 \approx 0$  in equation (53). The statistical error of the asymmetry is given by  $\sigma(A_{FB}) = \sqrt{1 - A_{FB}^2} / \sqrt{2N_{event}}$ , which results for the 2000 events of the data sample used

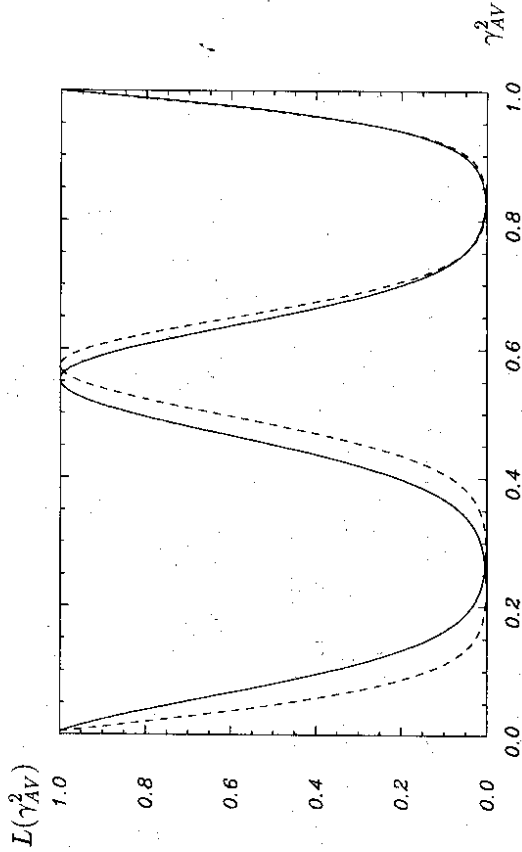


Figure 9: Likelihood function for three Monte Carlo samples with  $\gamma_{AV}^2 = 0.0, 0.6$  and  $1.0$  (without radiation effects) using an ideal detector. (full lines: average over the two reconstructed  $\tau$  axes; dashed lines: real  $\tau$  axis.)

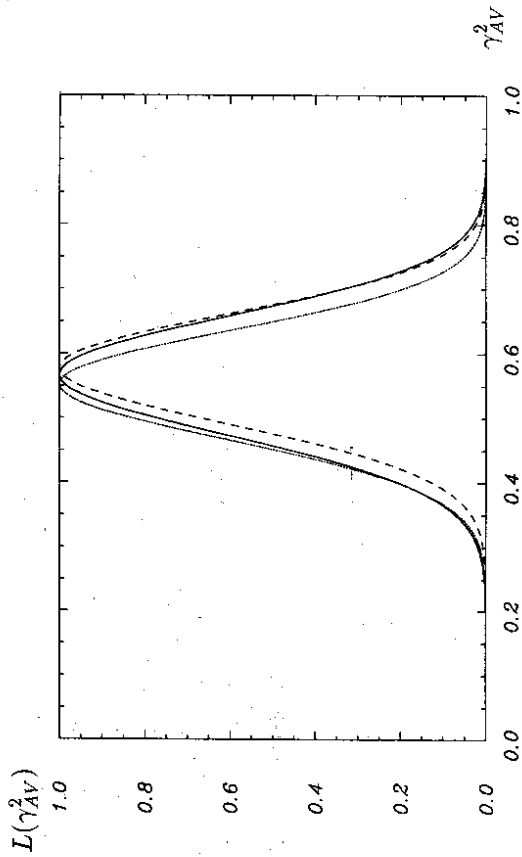


Figure 10: Comparison of likelihood functions for a real detector (full line) and for an ideal detector (dashed line) with radiation effects and an ideal detector without radiation effects (dotted line). (Input data:  $\gamma_{AV}^2 = 0.6$ )

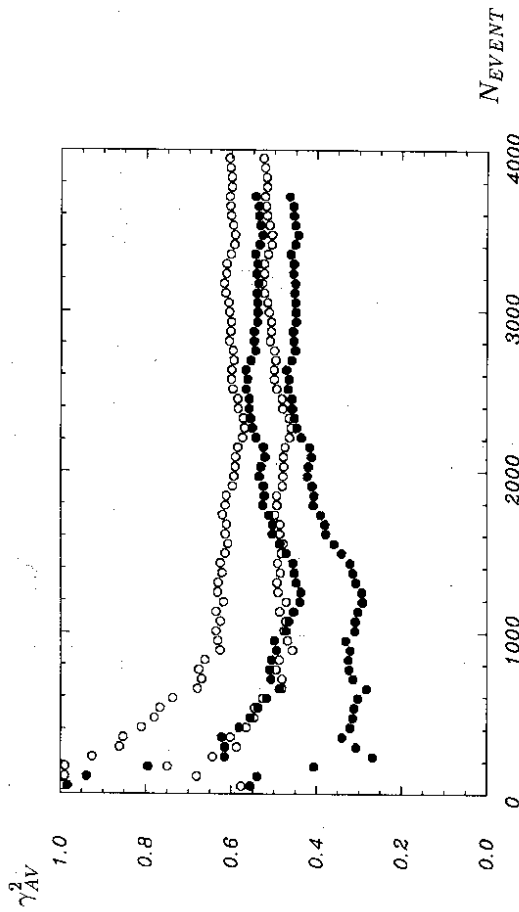


Figure 11: One-sigma boundaries for  $\gamma_{AV}^2$  depending on the number of analysed events for a real detector (full points) and an ideal detector (open points) (Input data:  $\gamma_{AV}^2 = 0.6$ ).

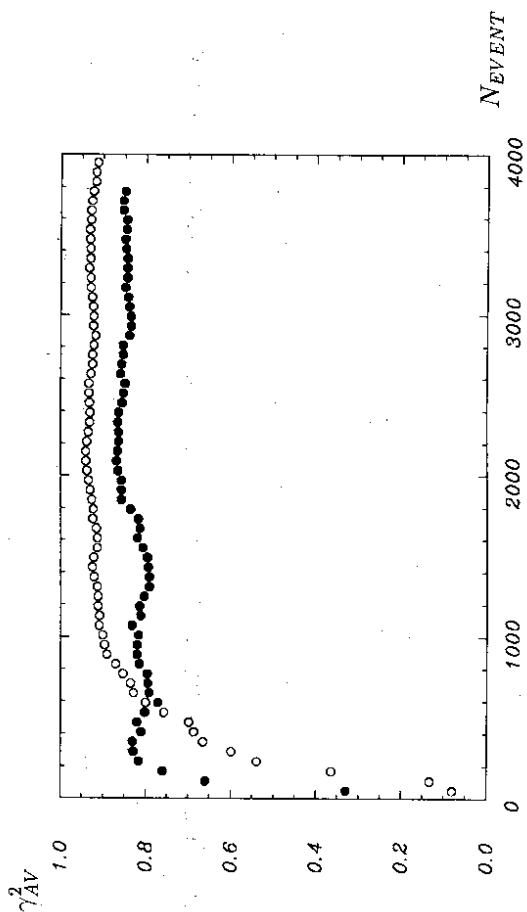


Figure 12: Lower limit (95% c.l.) for  $\gamma_{AV}^2$  depending on the number of analysed events for a real detector (full points) and for an ideal detector (open points) (Input data:  $\gamma_{AV}^2 = 1.0$ ).

method:	$\gamma_{AV}^2$ :	$\sigma(\gamma_{AV}^2)/0.6$ :
likelihood	$0.63 \pm 0.05$	8.3%
energy-energy correlation	$0.52 \pm 0.36$	60.0%
1-dim. distribution ( $\Sigma\phi$ )	$0.79 \pm 0.52$	86.7%

Table 1: Comparison of different methods to determine  $\gamma_{AV}^2$  using 2000 simulated events (input  $\gamma_{AV}^2 = 0.6$ ) and an ideal detector.

for table 1 in  $\sigma(\gamma_{AP}) = 0.034$  or  $|\gamma_{AP}| < 0.067$  at 95% c.l. Notice that the statistics is doubled by the fact that each event of reaction (2) contributes with  $\cos\alpha^-$  and  $\cos\alpha^+$ .

## 5 Summary

In summary, we have developed a method to determine the Lorentz structure of the electro-weak interaction in semi-hadronic  $\tau$  decays exploiting spin correlations in the process  $e^+e^- \rightarrow \tau^+\tau^- \rightarrow \bar{\nu}_\tau \pi^+\pi^0 \nu_\tau \pi^-\pi^0$ . The method requires the knowledge of the corresponding matrix element, which has been calculated and expressed in terms of angles and momenta of the measurable final state hadrons. The necessary reconstruction of the  $\tau$  direction of flight can be performed up to a twofold ambiguity. A likelihood method using the complete information of the matrix element has been outlined for the determination of  $\gamma_{AV}^2 = (2 \text{Re}\{g_{A9}g_V^*\})/(|g_V|^2 + |g_A|^2)^2$ . The sensitivity of this procedure has been checked with Monte Carlo data and the influence of the number of used events and of the finite detector resolution have been studied. Using projections of the fully differential cross section, such as energy-energy correlations in the final state hadron system, to determine  $\gamma_{AV}^2$  have also been tested. However, none of the methods was found to be competitive with the likelihood method. Finally, the contribution of a scalar-like coupling to the  $\tau$  decay amplitude has been investigated. The simple one-dimensional decay angular distribution of the two-pion system was found to be quite sensitive to such a coupling.

## A The $Z^0$ Contribution to the Production Amplitude

The calculation of the production amplitude  $P_{\lambda_+ \lambda_-}^{\lambda_+ \lambda_-}(e^+e^- \rightarrow Z^0 \rightarrow \tau^+\tau^-)$  is very similar to the one described in section 2, where the contribution of the one-photon exchange has been derived. Only two major changes have to be performed. At first one has to substitute the vertex factors by the ones for the  $Z^0$ -fermion-fermion coupling:

$$-ieQ_f\gamma^\mu \longrightarrow -ie\gamma^\mu(v_f - a_f\gamma^5) \quad (59)$$

with  $v_f = (I_3^f - 2\sin^2\theta_W Q_f)/(2\sin\theta_W \cos\theta_W)$  and  $a_f = I_3^f/(2\sin\theta_W \cos\theta_W)$ , where  $I_3^f$  is the third component of the weak isospin,  $\theta_W$  is the weak mixing angle and  $Q_f$  is the fermion charge. Secondly the  $Z^0$  propagator has to be used:

$$-i \frac{g_{\mu\nu}}{s} \longrightarrow -i \frac{F_Z}{s} \left( g_{\mu\nu} - \frac{q_\mu q_\nu}{M_Z^2} \right) \quad (60)$$

with  $F_Z = s/(s - M_Z^2 + iM_Z\Gamma_Z)$  and  $q = p_{\tau^+} + p_{\tau^-} = p_{e^+} + p_{e^-}$ .

Then the amplitudes for a production via  $Z_0$  exchange are:

$$P_{\lambda_+ \lambda_-}^{\lambda_+ \lambda_-}(e^+e^- \rightarrow Z^0 \rightarrow \tau^+\tau^-) = \bar{v}_e(\vec{p}_{e^+}, \lambda_{e^+})(-ie\gamma^\mu)(v_e - a_e\gamma^5)u_e(\vec{p}_{e^-}, \lambda_{e^-}) g_{\mu\nu} \quad (61)$$

$$(-i \frac{F_Z}{s}) \bar{v}_\tau(\vec{p}_{\tau^-}, \lambda_{\tau^-})(-ie\gamma^\nu)(v_\tau - a_\tau\gamma^5)v_\tau(\vec{p}_{\tau^+}, \lambda_{\tau^+}).$$

The resulting amplitudes for the various helicity combinations which have to be added to the one-photon exchange amplitudes in (6) to (9) are:

$$P_{+-}^{+-}(\theta_p) = -ie^2 F_Z (v_e - a_e)(v_\tau - a_\tau\beta_\tau)(\cos\theta_p + 1) \quad (62)$$

$$P_{-+}^{-+}(\theta_p) = -ie^2 F_Z (v_e + a_e)(v_\tau + a_\tau\beta_\tau)(\cos\theta_p + 1)$$

$$P_{+-}^{+-}(\theta_p) = -ie^2 F_Z (v_e + a_e)(v_\tau - a_\tau\beta_\tau)(\cos\theta_p - 1)$$

$$P_{-+}^{-+}(\theta_p) = -ie^2 F_Z (v_e - a_e)(v_\tau + a_\tau\beta_\tau)(\cos\theta_p - 1)$$

$$P_{-+}^{+-}(\theta_p) = ie^2 F_Z \frac{1}{\gamma} (v_e + a_e)v_\tau \sin\theta_p = -P_{+-}^{+-}(\theta_p)$$

$$P_{+-}^{-+}(\theta_p) = ie^2 F_Z \frac{1}{\gamma} (v_e - a_e)v_\tau \sin\theta_p = -P_{-+}^{-+}(\theta_p).$$

## B The Matrix Element in a Lorentz Invariant Formulation

The result of section 2.3 can be compared with the squared matrix element written in a Lorentz invariant way, which is given in appendix A (equation A.1-A.3) of reference [6], evaluated for the case of unpolarized beams and a pure one-photon exchange:<sup>4</sup>

$$A = \frac{G_F^4}{4} \frac{C_+ C_- |^2}{|C_+ C_-|^2} \frac{\omega_+ \omega_-}{s^2} (s^2 + (\Delta\Delta_\tau)^2 + 4sm_\tau^2) \quad (63)$$

$$\gamma_{AV}^2 B = \frac{G_F^4}{4} \frac{C_+ C_- |^2}{|C_+ C_-|^2} \frac{2}{s^2} \left\{ \left( 2 + \frac{s - 2m_\tau^2}{m_\tau^2} \right) [(PR_+)(PR_-) - (\Delta R_+)(\Delta R_-)] \right. \quad (64)$$

$$\left. + \frac{((\Delta\Delta_\tau)^2 - s^2 + 4sm_\tau^2)}{2m_\tau^2} \frac{R_+ R_-}{2m_\tau^2} + \frac{\Delta\Delta_\tau}{m_\tau^2} [(PR_+)(\Delta R_-) - (PR_-)(\Delta R_+)] \right\}$$

with:

$$\omega_\pm = P_{\tau^\pm}^\mu (\Pi_\mu^\pm - \gamma_{AV} \Pi_{5,\mu}^\pm) \quad (65)$$

$$= 2 |F_\tau(Q^2)|^2 [2(P_{\tau^\pm} q_\pm)(P_\nu q_\pm) - (P_{\tau^\pm} P_\nu) q_\pm^2],$$

$$R_\mu^\pm = (m_\tau^2 g^{\mu\lambda} - P_{\tau^\pm}^\mu P_{\tau^\pm}^\lambda) (\gamma_{AV} \Pi_\mu^\pm - \Pi_{5,\mu}^\pm) \quad (66)$$

$$= \gamma_{AV} 2 |F_\tau(Q^2)|^2 (m_\tau^2 g^{\mu\lambda} - P_{\tau^\pm}^\mu P_{\tau^\pm}^\lambda) [2q_\lambda^\pm (P_\nu q_\pm) - P_\nu^\lambda q_\pm^2],$$

$P = P_{e^+} + P_{e^-}$ ,  $\Delta = P_{e^+} - P_{e^-}$  and  $\Delta_\tau = P_{\tau^+} - P_{\tau^-}$ . For the reaction (2) we have used  $\Pi_{5,\mu}^\pm = 0$  and

$$\Pi_\mu^\pm = 4 \text{Re}\{(P_\nu J_{h^\pm}^\mu) J_{h^\pm}^{\mu\lambda}\} - 2 |J_{h^\pm}^\mu|^2 P_\nu^\mu$$

<sup>4</sup>The bold faced parts of the equation (64) are erroneously missing in reference [6].

with the hadronic current  $J_{h\pm}^\mu = F_\tau^h(Q^2) q_\pm^\mu$ .

## Acknowledgements

We want to thank Drs. D. Wyler and J.G. Körner for stimulating discussions and the ARGUS collaboration for supporting us with the detector simulation software.

## References

- [1] Reviews are given in:  
A. Pich (CERN), *Tau Physics*, CERN-TH-6237-91, Sep 1991, to appear in *Heavy Flavours*, ed. by A.J. Buras and M. Lindner, World Scientific, 1991;  
C. Kiesling, in "High Energy Electron-Positron Physics", eds. A. Ali, P. Söding, Singapore: World Scientific (1989) 177;  
B.C. Barish, R. Stroynowski, *Phys. Rep.* **157** (1988) 1.
- [2] M. Davier, Summary talk given at the 2<sup>nd</sup> Workshop on Tau Lepton Physics, Ohio (USA 1992), to appear in the proceedings and Orsay preprint LAL 92-74.
- [3] H. Albrecht et al. (ARGUS), *Phys.Lett.* **B246** (1990) 278;  
H. Jansen et al. (Crystal Ball), *Phys.Lett.* **B228** (1989) 273;  
S. Behrends et al. (CLEO), *Phys. Rev.* **D32** (1985) 2468.
- [4] H. Albrecht et al. (ARGUS), *Z. Phys. C.* **56** (1992) 339.
- [5] H. Albrecht et al. (ARGUS), *Phys.Lett.* **B250** (1990) 164.
- [6] J.H. Kühn and F. Wagner, *Nucl. Phys.* **B236** (1984) 16.
- [7] S. Jadach and Z. Was, "Monte Carlo Simulation of the Process  $e^+e^- \rightarrow \tau^+\tau^-, \tau^\pm \rightarrow X^\pm$  Including Radiative O ( $\alpha^3$ ) QED Corrections, Mass and Spin Effects", *Comp. Phys. Commun.* **36** (1985) 191;  
S. Jadach and Z. Was, "KORALB Version 2.1 - An Upgrade with TAUOLA Library of  $\tau$  Decays", *Comp. Phys. Commun.* **64** (1991) 267;  
S. Jadach, J.H. Kühn and Z. Was, "TAUOLA - A Library of Monte Carlo Programs to Simulate Decays of Polarized  $\tau$  Leptons", *Comp. Phys. Commun.* **64** (1990) 275.
- [8] S. Jadach, B.F.L Ward and Z. Was, "The Monte Carlo Program KORALZ, Version 3.8, for the Lepton or Quark Pair Production at LEP/SLC Energies", *Comp. Phys. Commun.* **66** (1991) 276.
- [9] H. Albrecht et al. (ARGUS), *Nucl.Instr.Meth.* **A275** (1989) 1.
- [10] H. Genow, "SIMARG: A Program to simulate the ARGUS detector", DESY internal report, DESY F15-85-02 (1985).
- [11] Z. Was, private communication (1993).
- [12] H. Thurn, Doctoral thesis, Universität Dortmund, in preparation.